Energy- and Electron-Transfer Processes Involving Palladium Porphyrins Bound to DNA

Anne M. Brun and Anthony Harriman*

Contribution from the Center for Fast Kinetics Research, The University of Texas at Austin, Austin, Texas 78712

Received June 15, 1994®

Abstract: The interaction of a series of isomeric palladium tetrakis(*N*-methyl-*x*-pyridinium)porphyrins (x = 2, 3, and 4) with DNA and synthetic polynucleotides has been studied. Both intercalation between base pairs (x = 3 and 4) and electrostatic binding to the external phosphate chain (x = 2) are observed. Once bound to DNA, the excited triplet state of these cationic porphyrins can be quenched by oxygen dissolved in the surrounding aqueous reservoir and by methyl viologen bound to the phosphate chain. Rates of quenching can be related to the location of the bound porphyrin on the DNA duplex. Singlet and triplet energy transfer is also observed from intercalated acridine orange to a porphyrin (x = 3) that is intercalated into the same helix. The rates of singlet energy transfer are discussed in terms of competing Förster- and Dexter-type mechanisms, and it is concluded that the DNA duplex does not provide a particularly attractive medium for electron exchange.

Many of the synthetic drugs in current usage, especially those used for radiation sensitization therapy of cancer, are targeted to react at cellular DNA.[1] In cases where the therapeutic mechanism involves electron transfer, it is necessary to consider the possibility that such electron transfer could occur over very large distances,[2] either by rapid diffusion of cationic species bound to the external phosphate chain[3] or by way of electron transfer through the interspersed base pairs.[4] Unambiguous experimental evidence for the latter process is lacking, although certain systems do appear to demonstrate long-range electron transfer between intercalated reagents.[4−6] Critical evaluation of the ability of DNA to mediate long-range electron (or energy) transfer, therefore, is an important part of the rational design of new therapeutic reagents. In particular, it is necessary to quantify the attenuation factor characteristic of electron transfer through the base pairs, since this relates to the distance over which a reaction can occur within a fixed time period. Previously, we determined that the attenuation factor for electron transfer through DNA was of the order of 0.9 $Å^{-1}$ for specific redox pairs.[4] A much lower value (i.e., <0.2 $Å^{-1}$) was obtained for a different redox couple separated by a significantly larger distance.[6] In extending this work, we now consider electron transfer occurring *via* migration along the phosphate chain and also describe the corresponding energy-transfer processes. In the event of an unusually low attenuation factor we might expect singlet energy transfer *via* a Dexter mechanism to compete with Förster-type transfer for intercalated species.

To this end, we have studied the interaction between DNA and a series of palladium porphyrins. Cationic porphyrins based on the tetrakis(*N*-methyl-*x*-pyridinium)porphyrin tetrachloride (with x = 2, 3, or 4) subunit have been used. For these compounds it is recognized that the position of the methyl substituent on the pyridinium ring, and therefore the stereochemistry of the porphyrin, allows for either intercalation into DNA or external binding to the phosphate chain.[7,8] A negatively-charged porphyrin based on tetrakis(4-sulfonatophenyl)porphyrin does not bind to DNA, either by intercalation or external binding, because of strong electrostatic repulsion, and has been used as a control. Distinction between the various binding modes is conveniently made by monitoring the triplet lifetime since oxygen diffuses at quite disparate rates to porphyrin molecules localized at different binding sites. Reaction of the triplet state of these porphyrins with various quenchers can be used to elicit kinetic information about diffusional quenching processes.

In order to address the issue of energy transfer along the DNA duplex, Acridine Orange was used as an energy donor. This heterocycle readily intercalates into DNA[9] and, from its spectroscopic properties, is expected to transfer both singlet and triplet excitation energy to the above palladium porphyrins. These studies allow us to monitor both Förster[10] and Dexter[11] energy-transfer processes between compounds intercalated into DNA and to assess the role of DNA in mediating these reactions. Because of the similarity between electron transfer and Dexter-type energy transfer, these studies also help address the

® Abstract published in *Advance ACS Abstracts*, October 15, 1994.

(1) Hill, B. T. *Cancer Treatment Rev.* **1991**, *18*, 149.

(2) (a) Fielden, E. M.; Lilicrap, S. C.; Robins, A. B. *Radiation Res.* **1971**, *48*, 421. (b) Whillans, D. W. *Biochim. Biophys. Acta* **1975**, *414*, 193. (c) Gräslund, A.; Ehrenberg, A.; Ström, G.; Crespi, H. *Int. J. Radiation Res.* **1975**, *28*, 313. (d) Gregoli, S.; Olast, M.; Bertinchamps, A. *Radiation Res.* **1982**, *89*, 238. (e) van Lith, D.; Warman, J. M.; de Haas, M. P.; Hummel, A. *J. Chem. Soc., Faraday Trans. 1* **1986**, *82*, 2933; 2945.

(3) (a) Atherton, S. J.; Beaumont, P. C. *J. Phys. Chem.* **1986**, *90*, 2252. (b) Atherton, S. J., Beaumont, P. C. *J. Am. Chem. Soc.* **1987**, *91*, 3993.

(4) Brun, A. M.; Harriman, A. *J. Am. Chem. Soc.* **1992**, *114*, 3656.

(5) (a) Baguley, B. C.; Denny, W. A.; Atwell, G. J.; Cain, B. F. *Eur. J. Cancer* **1981**, *6*, 671. (b) Baguley, B. C.; Cain, B. F. *Mol. Pharmacol.* **1982**, *22*, 486. (c) Baguley, B. C.; Le Bret, M. *Biochemistry* **1984**, *23*, 937.

(6) Murphy, C. J.; Arkin, M. R.; Jenkins, Y.; Ghatlia, N. D.; Bossman, S. H.; Turro, N. J.; Barton, J. K. *Science* **1993**, *262*, 1025.

(7) (a) Pasternack, R. F.; Gibbs, E. J.; Gaudemer, A.; Antebi, A., Bassner, S.; De Poy, L.; Turner, D. H.; Williams, A.; Laplace, F.; Lansard, M. H.; Merienne, C.; Perrée-Fauvet, M. *J. Am. Chem. Soc.* **1985** *107*, 8179. (b) Pasternack, R. F.; Brigandi, R. A.; Abrams, M. J.; Williams, A. P.; Gibbs, E. J. *Inorg. Chem.* **1990**, *29*, 4483. (c) Pasternack, R. F.; Caccam, M.; Keogh, B.; Stephenson, T. A.; Williams, A. P.; Gibbs, E. J. *J. Am. Chem. Soc.* **1991**, *113*, 6835. (d) Pasternack, R. F.; Bustamante, C.; Collings, P. J.; Giannetto, A.; Gibbs, E. J. *J. Am. Chem. Soc.* **1993**, *115*, 5393 and references therein.

(8) (a) Strickland, J. A.; Marzilli, L. G.; Gary, K. M.; Wilson, W. D. *Biochemistry* **1988**, *27*, 8870. (b) Strickland, J. A.; Banville, D. L.; Wilson, W. D.; Marzilli, L. G. *Inorg. Chem.* **1987**, *26*, 3398. (c) Kelly, J. M.; Murphy, M. J.; McConnell, D. J.; OhUigin, C. *Nucleic Acid Res.* **1985**, *13*, 167. (d) Slama-Schwok, A.; Lehn, J.-M. *Biochemistry* **1990**, *29*, 7895.

(9) (a) Müller, W.; Crothers, D. *Eur. J. Biochem.* **1975**, *54*, 267. (b) Löber, G.; Achtert, G. *Biopolym.* **1969**, *8*, 595. (c) Löber, G. *J. Luminescence* **1981**, *22*, 221. (d) Kittler, L.; Löber, G.; Goolmich, F. A.; Berg, H. *Bioelectrochemistry Bioenergetics* **1980**, *7*, 502.

(10) Förster, T. *Discuss. Faraday* **1959**, *27*, 7.

(11) Dexter, D. L. *J. Chem. Phys.* **1953**, *21*, 836.

0002-7863/94/1516-10383$04.50/0

Chart 1

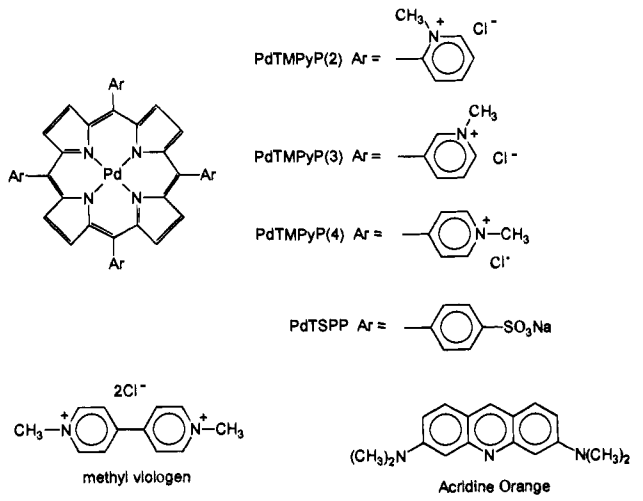

intriguing question of the mechanism of electron-transfer reactions in DNA.

Experimental Section

Salts of the following palladium porphyrins were obtained from Mid-Century and were used without further purification: Pd(II)TMPyP(x) (with x = 2, 3, or 4) where TMPyP(x) is meso-tetrakis(N-methyl-x-pyridinium)porphyrin tetrachloride. The negatively-charged palladium tetrakis(4−sulfonatophenyl)porphyrin, sodium salt (PdTSPP) was included in the series for comparative purposes. Porphyrin concentrations were determined from the absorbance at the respective Soret maxima, recorded in dilute aqueous solution, using the following molar extinction coefficients: $\epsilon = 158 \times 10^3$ M^{-1} cm^{-1} (@ 417 nm) for PdTMPyP(4); $\epsilon = 154 \times 10^3$ M^{-1} cm^{-1} (@ 412 nm) for PdTMPyP-(3); $\epsilon = 150 \times 10^3$ M^{-1} cm^{-1} (@ 408 nm) for PdTMPyP(2); and $\epsilon = 156 \times 10^3$ M^{-1} cm^{-1} (@ 410 nm) for PdTSPP. Acridine Orange (Aldrich Chem.) was chromatographed on silica gel with a mixture of butan-1-ol/trifluoroacetic acid/water = 8:2:1 as eluent: $\epsilon = 57 \times 10^3$ M^{-1} cm^{-1} at 492 nm in aqueous buffer. Calf-thymus deoxyribonucleic acid, sodium salt (DNA) was purchased from Sigma Chem. Co. and was purified by phenol extraction and dialysis. Stock solutions of DNA were prepared by dissolution overnight in 5 mM phosphate buffer (pH = 7) and were stored at 4 °C in the dark for short periods only. Concentrations of DNA per nucleotide phosphate were determined by absorption spectroscopy using a molar extinction coefficient of 6600 M^{-1} cm^{-1} at 260 nm.[12] Samples of double-stranded copolymer consisting of alternating deoxyadenylic acid and deoxythymidylic acid, sodium salt ([poly(dAdT)]$_2$) and of deoxyguanylic acid and deoxycytidilic acid, sodium salt ([poly(dGdC)]$_2$) were obtained from Sigma Chem. Co. and were stored at 0 °C. Concentrations of these polynucleotides, measured in terms of nucleotide phosphate, were determined using molar extinction coefficients at 260 nm of 6600 and 8400 M^{-1} cm^{-1}, respectively, for [poly(dGdC)]$_2$ and [poly(dAdT)]$_2$.[13] Water was distilled fresh from a Millipore Q system.

Absorption spectra were recorded with a Hitachi U3210 spectrophotometer and fluorescence spectra were recorded with a fully-corrected Perkin-Elmer LS5 spectrofluorimeter. The excitation wavelength was 408 nm for PdTMPyP(2) and PdTMPyP(3), 418 nm for PdTMPyP(4), 410 nm for PdTSPP, and 490 nm for AO. The spectra were recorded at room temperature in phosphate buffer (5 mM, pH = 7) with or without polynucleotide, and, unless stated otherwise, the solutions were air-equilibrated. Absorbances at the excitation wavelength were 0.05 or less. Binding constants were determined from absorption and emission spectral changes, measurements being made by adding increasing amounts of polynucleotide solution to a buffered solution of dye and *vice versa*. At least 15 different concentrations of substrate were used for each titration.

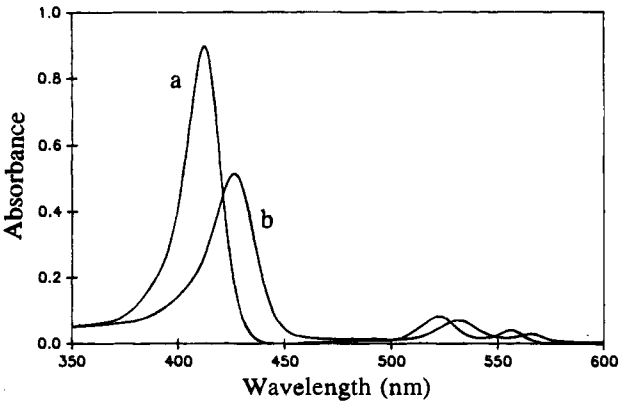

Figure 1. Absorption spectra of PdTMPyP(3) recorded in (a) neutral aqueous solution and (b) the presence of DNA at a P/D of 40.

Energy-transfer studies were made with a time-correlated, single-photon counting instrument using a mode-locked Nd-YAG synchronously-pumped, cavity-dumped Styryl-9 dye laser (FWHM = 6 ps). The laser output was frequency-doubled (λ = 440 nm) so as to selectively excite Acridine Orange (AO). Fluorescence was separated from scattered laser light with a high radiance monochromator and was monitored at several wavelengths within the range 520−560 nm with a fast response (rise time 40 ps) microchannel plate phototube. Titrations were carried out by adding successive amounts of an aqueous solution of PdTMPyP(3) to a freshly-prepared DNA stock solution containing a fixed concentration of AO ([AO] = 10 μM, [DNA phosphate] = 200 μM) in air-equilibrated solution. After deconvolution of the instrument response function and applying global analysis methodology, the ultimate time resolution of this instrument was *ca.* 20 ps. All reported lifetimes had a reproducibility better than 5%. Each titration was repeated several times, and the quoted lifetimes are the averages of several data sets.

Laser flash photolysis studies were made with a frequency-doubled (λ = 532 nm for excitation of palladium porphyrins) or frequency-tripled (λ = 355 nm for excitation of AO) Nd-YAG laser. The laser was Q-switched and a pulsed Xe arc lamp was used as monitoring beam. The laser intensity was attenuated when needed with metal screen filters. Spectra were recorded point-by-point with five individual records being computer-averaged at each wavelength. Kinetic studies were made at fixed wavelength, with 50 individual records being averaged at each time base, baseline corrected, and analyzed by computer iteration. Solutions had an absorbance of 0.2 at the excitation wavelength and were purged thoroughly with N_2 before and during the experiment. Phosphorescence decay profiles were recorded at 690 nm for the various palladium porphyrins in deoxygenated solution.

Singlet molecular oxygen was detected by time-resolved luminescence spectroscopy at 1270 nm.[14] Solutions of porphyrins in D_2O were adjusted to possess an absorbance at 532 nm of *ca.* 0.2 and were saturated with O_2. The solutions were irradiated with single 10-ns pulses from a frequency-doubled Nd:YAG laser and emission was detected at 90° using a filtered Ge diode detector. Laser intensities were attenuated using neutral density filters, and the yield of singlet oxygen was derived by computer extrapolation of the first-order decay profile to the center of the laser pulse. For each record, 20 individual laser shots were averaged and analyzed by computer nonlinear least-squares iteration.

Results and Discussion

Interaction with DNA. The effect on the visible absorption spectrum of adding a large excess of DNA to a solution of PdTMPyP(3) is shown in Figure 1. The absorption peaks observed in the presence of excess DNA were shifted and somewhat broadened relative to those in water; the shifts in the Soret band peak position for PdTMPyP(x) with x = 2, 3, or

(12) Reichmann, M. E.; Rice, S. A.; Thomas, C. A.; Doty, P. J. *J. Am. Chem. Soc.* **1954**, *76*, 3047.

(13) Kelly, J. M.; van der Putten, W. J. M.; McConnell, D. J. *Photochem. Photobiol.* **1987**, *45*, 167.

(14) Rodgers, M. A. J.; Snowden., P. T. *J. Am. Chem. Soc.* **1982**, *104*, 5341.

Table 1. Interaction between Nucleic Acids and the Various Palladium Porphyrins[f]

porphyrin	$K/10^5$ [a] (M^{-1})	water[b] λ_{max}/nm	DNA[c] λ_{max}/nm	[dGdC][d] λ_{max}/nm	[dAdT][e] λ_{max}/nm
PdTMPyP(2)	4.3	408	411(8)	412(9)	411(5)
PdTMPyP(3)	6.3	412	426(43)	425(47)	422(33)
PdTMPPyP(4)	1.2	417	434(42)	434(48)	425(19)
PdTSPP	<0.1	410	410(0)	410(0)	410(0)

[a] Binding constant for interaction between the porphyrin and DNA ±5%. [b] Soret band absorption maximum (and hypochromicity) in water, ±2 nm. [c] Soret band absorption maximum (and hypochromicity) in DNA at P/D = 40, ±2 nm. [d] Soret band absorption maximum (and hypochromicity) in $[poly(dGdC)]_2$ at P/D = 40, ±2 nm. [e] Soret band absorption maximum (and hypochromicity) in $[poly(dAdT)]_2$ at P/D = 40, ±2 nm. [f] Spectroscopic data refer to a P/D ratio of 40, and the percentage of hypochromicity is given in parentheses after the absorption maximum.

4 are reported in Table 1 for a fixed phosphate/dye ratio (P/D) of 40. As expected from the comprehensive work of Pasternack[7] and others,[8] PdTMPyP(3) and PdTMPyP(4) exhibited a substantial red shift in the Soret band maximum (14 and 17 nm, respectively) and a pronounced hypochromicity (i.e., ≈40%). In contrast, PdTMPyP(2) showed a red shift of only 3 nm with the extinction coefficient being only slightly reduced, while for PdTSPP the absorption spectrum was unaffected by addition of excess DNA. The Q bands of the various porphyrins also exhibited comparable shifts upon addition of DNA; those for PdTMPyP(3) and PdTMPyP(4) being red shifted by 10 and 12 nm, respectively, while those for PdTMPyP(2) and PdTSPP were not noticeably affected.

The influence of the synthetic polymers $[poly(dGdC)]_2$ and $[poly(dAdT)]_2$ on the absorption spectra was also examined. The respective shifts in the Soret band peak position are listed in Table 1. The addition of $[poly(dGdC)]_2$ caused comparable spectral changes to those observed with DNA, whereas the addition of $[poly(dAdT)]_2$ had less effect on either the position of the absorption maxima or the magnitude of the molar extinction coefficients for any of the porphyrins. These findings are consistent with both PdTMPyP(3) and PdTMPyP(4) exhibiting modest preference for intercalation at GC rich regions on the DNA duplex.

All the available experimental evidence indicates that PdTSPP does not bind to DNA or to the synthetic polynucleotides, presumably due to strong electrostatic repulsion. Because of steric crowding between pyrrole and methyl groups, the pyridinium ring in PdTMPyP(2) cannot become coplanar with the porphyrin nucleus. This hinders intercalation of a porphyrin molecule between base pairs comprising the duplex[15] and, based on the modest spectral shifts, virtual absence of hypochromicity, and greater accessibility of PdTMPyP(2) to species free in solution or bound to the phosphate chain (see later), it is most likely that this compound binds to the exterior of the DNA helix *via* electrostatic forces. The binding constant for this process was found to be $(4.3 \pm 0.7) \times 10^5$ M^{-1}, while the saturation number corresponds to one molecule of porphyrin occupying three base pairs. In contrast, the large spectral shifts, extensive hypochromicity, protection against species in solution, and induced circular dichroism observed for PdTMPyP(3) and PdTMPyP(4) are consistent with these porphyrins being intercalated into DNA. The binding constants were found to be similar to that found for PdTMPyP(2) (Table 1), and, from McGhee–von Hippel plots,[16] these latter isomers occupy two base pairs. Both PdTMPyP(3) and PdTMPyP(4), but not

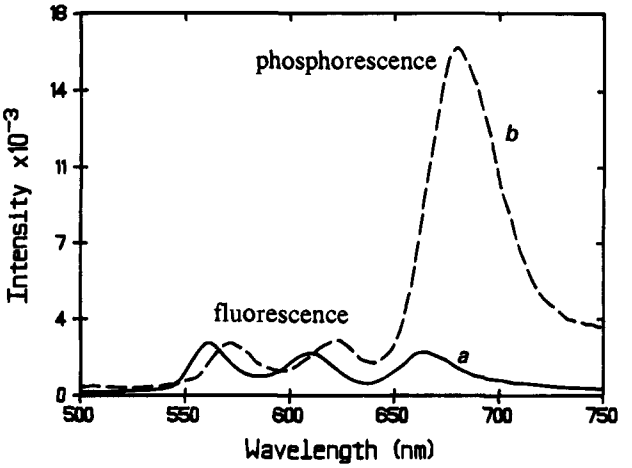

Figure 2. Luminescence spectra of PdTMPyP(3) recorded in (a) neutral aqueous solution and (b) the presence of DNA at a P/D of 40.

PdTMPyP(2) nor PdTSPP, unwind covalently-closed, superhelical DNA and demonstrate a definite, albeit modest, preference for G–C rich environments. Time-resolved luminescence and transient absorption studies do not support the notion of mixed binding sites for these cationic porphyrins since the decay records could be analyzed satisfactorily in terms of single-exponential components at P/D ≈ 40. Thus, it appears that, at low loadings, the porphyrins either intercalate between base pairs or bind to the exterior of the duplex.

Oxygen Quenching of Excited Triplet States. Excitation of PdTMPyP(*x*) in aqueous solution gives rise to very weak fluorescence and phosphorescence at ambient temperature. The emission spectrum of each porphyrin was recorded, in air-equilibrated aqueous solution, in the presence of a large excess of DNA, $[poly(dGdC)]_2$, or $[poly(dAdT)]_2$; the effect of DNA on the emission spectrum of PdTMPyP(4) is shown in Figure 2. For each porphyrin in air-equilibrated solution, interaction with the biopolymer caused a substantial enhancement of the phosphorescence emission compared to that of the porphyrin in aqueous solution; the fluorescence quantum yield remaining constant after normalization of the absorbance at the excitation wavelength.[17] The ratio of the phosphorescence yields measured in water and in DNA for each porphyrin, under air-equilibrated conditions, is given in Table 2, and it can be seen that PdTMPyP(3) and PdTMPyP(4) show more pronounced enhancement of the phosphorescence quantum yield than does PdTMPyP(2). Again, these findings are entirely consistent with the former porphyrins intercalating into the duplex, and thereby being protected against quenching by O_2 dissolved in the aqueous reservoir, with the latter porphyrin being bound to the external phosphate chain.

The triplet excited state of these porphyrins in N_2-saturated, neutral aqueous solution could be observed readily after excitation with a 10-ns laser pulse at 532 nm. The triplet differential absorption spectra were similar for all compounds. For [PdTMPyP(*x*)] = 5 μM and [DNA] = 200 μM (P/D = 40), the triplet state decayed by first-order kinetics and the lifetimes measured under N_2 are reported in Table 2. The bimolecular rate constants for quenching the various triplets by O_2 (k_Δ) were determined from the first-order rate constant for decay of the triplet as a function of the concentration of dissolved oxygen using calibrated mixtures of N_2 and O_2. The respective values are collected in Table 2 as well as the ratio of the rate constants measured in water and in DNA, k_w/k_{DNA}. In

(15) Saenger, W. In *Principles of Nucleic Acid Structure*; Cantor, C. R., Ed.; Springer-Verlag: New York, 1984.
(16) McGhee, J. D.; Von Hippel, P. H. *J. Mol. Biol.* **1974**, *86*, 469.
(17) The fluorescence lifetimes recorded for the various palladium porphyrins in deoxygenated aqueous solution were *ca.* 100 ps and remained unaffected upon saturation of the solution with O_2.

Table 2. Triplet Lifetimes and Bimolecular Rate Constants for Quenching the Various Porphyrin Triplet Excited States by Oxygen in Water and in the Presence of Polynucleotides (P/D = 40)

porphyrin	τ_t^a (μs)	k_Δ^b 10^9 M^{-1} s^{-1}	τ_t^c (μs)	k_w/k_{DNA}^d	τ_t^e (μs)	I_{DNA}/I_w^f
PdTMPyP(2)	105	1.6	125	3.6	8.1	2.5
PdTMPyP(3)	100	1.2	360	21.2	47.2	8.0
PdTMPyP(4)	115	2.2	350	22.3	48.0	7.1
PdTSPP	205	2.3	205	1.0	2.3	1.0

[a] Triplet lifetime measured in deoxygenated water. [b] Bimolecular rate constant for quenching the triplet state by O_2 in water. [c] Triplet lifetime measured in deoxygenated water in the presence of DNA (P/D = 40). [d] Ratio of the bimolecular rate constants for quenching the triplet state by O_2 in water in the absence and presence of DNA (P/D = 40). [e] Triplet lifetime measured in air-equilibrated water in the presence of [poly(dGdC)]$_2$ (P/D = 40). [f] Ratio of phosphorescence quantum yields measured in air-equilibrated DNA (P/D = 40) and water.

the case of PdTSPP, which does not bind to DNA, the rate constants in water and in DNA are identical (i.e., k_w/k_{DNA} = 1). The large ratio of k_w/k_{DNA} noted for PdTMPyP(3) and PdTMPyP(4) reflects the relative inability of oxygen to diffuse to a porphyrin that is intercalated into the DNA strand. As such, PdTMPyP(2), which binds to the exterior of the double helix, shows behavior intermediate between these two extremes. This porphyrin is not "protected" by the DNA helix as much as are the other isomers but, due to external binding, k_w exceeds k_{DNA}. Similar results were obtained with [poly(dGdC)]$_2$.

For PdTMPyP(3), decay of the triplet excited state was studied as a function of the P/D ratio, for [DNA] = 200 μM and [PdTMPyP(3)] = 0−25 μM. In air-equilibrated water (P/D = 0), or with excess DNA (P/D >25), the triplet decayed by first-order kinetics. However, for P/D ratios between these two extremes, the kinetic profiles were best described with a two exponential fit: $I(t) = A_1 \exp(-t/\tau_1) + A_2 \exp(-t/\tau_2)$. The derived lifetimes (τ_1 = (2.3 ± 0.4) μs and τ_2 = (25 ± 5) μs) did not change with increasing concentration of DNA, but the ratio A_2/A_1 increased with increasing P/D. The faster decaying process (τ_1) is ascribed to porphyrin that remains free in solution, while the slower decaying species is attributed to intercalated porphyrin. Indeed, using the binding constant derived from absorption spectral changes, the ratio of "fast" and "slow" components in the triplet decay records could be explained quantitatively in terms of free and intercalated dye.

The above conclusions were supported by time-resolved luminescence studies in which the resultant singlet molecular oxygen, formed *via* triplet energy transfer from a palladium porphyrin to O_2, was monitored. It was observed that each of the porphyrins gave a comparable quantum yield for production of singlet molecular oxygen ($\Phi_\Delta \approx 0.80$), but the time scale for formation of singlet oxygen was dependent upon the location of the porphyrin. Thus, in air-equilibrated D_2O formation of singlet oxygen was complete within 4 μs for each porphyrin; singlet oxygen subsequently decayed with a lifetime of *ca.* 55 μs. The presence of DNA (P/D = 40) had no effect on the rate of formation of singlet oxygen for PdTSPP, but for PdTMPyP-(2) singlet oxygen was observed to be generated with a first-order rate constant of (1.1 ± 0.2) × 10^5 s^{-1}. Formation of singlet oxygen occurred with a first-order rate constant of (4.0 ± 0.5) × 10^4 s^{-1} for the two intercalated porphyrins. These results are consistent with the stated ability of DNA to protect PdTMPyP(3) and PdTMPyP(4) from species free in solution.

Electron-Transfer Processes. Methyl viologen (MV^{2+}) was found to quench the triplet lifetime of each of the cationic palladium porphyrins in neutral aqueous solution; extensive ion-pairing occurs between MV^{2+} and the negatively-charged PdTSPP[18] which precludes such experiments being made in this case. At an ionic strength of 0.05 M, as adjusted by addition of KCl, the bimolecular quenching rate constants (k_Q) were determined by monitoring the effect of successive additions of MV^{2+} on the triplet lifetime in deoxygenated solution. The derived values are collected in Table 3 and are seen to be well below the diffusion-controlled rate limit. Because of the ionic nature of the reactants, these bimolecular rate constants were markedly dependent on ionic strength (μ) and conformed to the Debye−Huckle equation in its simplest form

Table 3. Quenching of the Triplet Excited State of the Cationic Palladium Porphyrins by Methyl Viologen in Water

x	$k_Q/10^6$ (M^{-1} s^{-1})	$k_o/10^5$ (M^{-1} s^{-1})	z_Az_B	$k_{DIF}/10^9$ (M^{-1} s^{-1})
2	2.1	3.5	4.3	1.5
3	3.5	1.6	5.9	0.84
4	3.4	5.5	3.9	1.7

$$\log k_Q = \log k_o + 1.02 z_A z_B (\mu)^{1/2} \quad (1)$$

where k_o refers to the quenching rate constant at zero ionic strength. The z_Az_B terms, calculated from the slopes, were found to be significantly smaller than the maximum (expected) value of 8 (Table 3), presumably because of low activity coefficients for the various species. The observed trend in z_Az_B parameters can be explained in terms of the extent of localization of the cationic charge on the pyridinium ring of the porphyrinic molecule. Thus, resonance forms can be drawn for PdTMPyP-(4), that delocalize the positive charge over the pyridinium ring and onto the porphyrin nucleus.[19] This has the effect of lowering the apparent electronic charge on the molecule. In principle, similar resonance forms can be drawn for PdTMPyP-(2) but steric hindrance prevents the pyridinium ring from becoming fully coplanar with the porphyrin nucleus[19] and, consequently, there will be less tendency to push the positive charge onto the porphyrin ring. Hence, the effective local electronic charge density will be higher than that for PdTMPyP-(4). For PdTMPyP(3), the positive charge will be localized on the pyridinium ring, and this molecule displays the highest effective electronic charge. The same trend is observed for the redox potentials for one-electron reduction of the porphyrin in water[20] and, again, can be related to the electron density resident on the porphyrin nucleus.

The derived k_o values can be compared with the diffusion controlled bimolecular rate constants (k_{DIF}) calculated from the Debye equation for reaction between two cations with the relevant z_Az_B terms (Table 3). In this way, it is seen that an average of about 4000 encounters are needed before electron transfer takes place. This is a consequence, at least in part, of the poor thermodynamic driving force for light-induced electron transfer.[21]

$$^*\text{PdTMPyP(x)} + MV^{2+} \rightarrow \text{PdTMPyP(x)}^{\bullet+} + MV^{\bullet+} \quad (2)$$

$$\Delta G^\circ \approx -0.05 \text{ eV}$$

The formation of net electron-transfer products was confirmed in each case by detection of the respective π-radical cations

(18) Brun, A. M.; Harriman, A.; Hubig, S. M. *J. Phys. Chem.* **1992**, *96*, 254.

(19) Richoux, M. C.; Neta, P.; Christensen, P. A.; Harriman, A. *J. Chem. Soc., Faraday Trans. 2* **1986**, *82*, 235.

(20) Reduction potentials measured for PdTMPyP(x) in neutral aqueous solution were as follows: x = 2, E° = −0.78 V vs NHE; x = 3, E° = −0.90 V vs NHE; x = 4, E° = −0.68 V vs NHE. The reduction potential found for PdTSPP was −1.00 V vs NHE.

using laser flash photolysis techniques. Indeed, such reactions have been observed with several other metalloporphyrins.[22]

Methyl viologen was also found to quench the excited triplet states of the cationic palladium porphyrins in the presence of DNA; earlier work[23] has shown that MV^{2+} quenches the fluorescence of intercalated ethidium bromide. Thus, each of the porphyrins ([PdTMPyP(x)] = 5 μM) was incubated with DNA ([DNA phosphate] = 200 μM) at an ionic strength of 0.05 M. The luminescence spectrum was measured in air-equilibrated solution as a function of increasing concentration of MV^{2+}, and it was observed that, whereas the fluorescence yield was not affected by the presence of MV^{2+}, the phosphorescence yield decreased upon successive addition of viologen. Quenching did not follow conventional Stern–Volmer behavior but, in each case, corresponded to a one-dimensional diffusional process (Figure 3). For the two porphyrins that intercalate between base pairs (i.e., PdTMPyP(3) and PdTMPyP(4)), the extent of phosphorescence quenching could be expressed in the following form[23]

$$(\Phi_o/\Phi) - 1 = 1.8(4D\tau_p/\pi d^2)^{1/2}K\alpha[MV^{2+}] \qquad (3)$$

where Φ_o and Φ, respectively, are the phosphorescence yields in the absence and presence of a certain concentration of MV^{2+} (i.e., $[MV^{2+}]$), and τ_p is the phosphorescence lifetime measured in the absence of viologen. In this expression,[23] d refers to the distance between phosphate groups (d = 3.4 Å), D is the diffusion coefficient for bound viologen, K is the association constant that characterizes binding of viologen to DNA ($K = 1.8 \times 10^5$ M^{-1}),[23] and α is the saturation number for binding MV^{2+} to DNA (α = 1.0 per base pair).[23] Evaluation of this expression for the two intercalated porphyrins gave an effective diffusion coefficient for the viologen moiety of $(1.3 \pm 0.2) \times 10^{-13}$ cm^2 s^{-1}. This is much lower than the value derived previously ($D = 2.5 \times 10^{-7}$ cm^2 s^{-1})[23] and suggests that, as in fluid solution, a great number of encounters are necessary before electron transfer takes place.

For the two intercalated porphyrins, it is clear that quenching saturates at a viologen concentration of *ca.* 100 μM (Figure 3). This corresponds to complete occupancy of the phosphate groups by bound viologen. At this concentration, therefore, a viologen molecule is in very close proximity to the intercalated porphyrin, and the extent of quenching corresponds to the maximum rate of electron transfer (k_{max}). The derived rate constants are collected in Table 4 and are seen to be very low. Clearly, the DNA matrix does not accelerate the rate of electron transfer for this system and, in fact, the rate of electron transfer in DNA appears to be even slower than that in water. Thus, the first-order rate constant for electron transfer within the precursor complex formed by diffusive encounter between the reactants (k_{el}) can be expressed[24] as

$$k_{el} = k_o/K_p \qquad (4)$$

where K_p is the association constant for formation of the precursor complex. Assuming the latter has a value of *ca.* 1 M^{-1}, as expected on the basis of the respective molar volumes,[25] we can equate k_{el} with k_o. For the two intercalating porphyrins, k_{el} is at least 50-fold greater than k_{max}. This difference might arise from different thermodynamic driving forces, reorganization energies, or orientations for the two types of complex.

For PdTMPyP(2), which binds to the external phosphate chain in preference to intercalation, the profile of the phosphorescence yield *vs* viologen concentration plot is similar to those obtained for the other isomers at low loadings of viologen (Figure 3). However, phosphorescence quenching does not cease once all the phosphate groups are bound with a viologen molecule. This additional phosphorescence quenching process follows Stern-Volmer behavior (Figure 3) with a bimolecular rate constant of $(8.5 \pm 0.9) \times 10^8$ M^{-1} s^{-1}. It is attributed to quenching of surface-bound PdTMPyP(2) by viologen free in solution and is a consequence of the porphyrin being relatively accessible to the bulk solution. At saturation of the phosphate groups, phosphorescence quenching corresponds to a k_{max} value of $(1.2 \pm 0.2) \times 10^4$ s^{-1} and a diffusion coefficient for bound viologen of $(8.8 \pm 0.9) \times 10^{-13}$ cm^2 s^{-1} (Table 4). Again, the rate of electron transfer is slower than that calculated for a corresponding precursor complex formed in water. The rate is faster, however, than those found for the intercalated porphyrins, suggesting that the thermodynamic driving force and/or reorganization energy for surface-bound porphyrin more closely resembles the values in water.

Time-resolved studies were made in N_2-saturated solution for each of the PdTMPyP(x) species bound to DNA at a P/D of 40. In the absence of viologen, decay of the porphyrin excited triplet state could be fit to a first-order decay law with the lifetimes listed in Table 2. Upon addition of low concentrations of viologen the decay profiles became nonexponential but could be well represented by the following expression[26]

$$I_t(t) = I_o((k_p + k_m)t + k_t t^{1/2}) \qquad (5)$$

where k_p is the inherent triplet decay rate in the absence of viologen, k_m refers to the rate of migration of a viologen molecule along the phosphate chain, and k_t is the rate of electron transfer at the closest approach. The derived values are collected in Table 4, and it can be seen that k_t remains in good agreement with the corresponding k_{max} values extracted from the steady-state luminescence studies. These values confirm that electron transfer is inefficient, especially for intercalated porphyrins. The k_m values can be used to estimate the one-dimensional hopping rate[27] for viologen migrating along the phosphate chain (ν)

$$\nu = \pi(k_m)^2/8(X_{Pd})^2 \qquad (6)$$

where X_{Pd} refers to the mole fraction of PdTMPyP(x). The average value ($\nu \approx 3.5 \times 10^7$ s^{-1}) corresponds to an approximate diffusion coefficient of 2×10^{-8} cm^2 s^{-1}, which is in closer agreement with the literature value ($D = 2.5 \times 10^{-7}$ cm^2 s^{-1}).[23]

With sufficient viologen to saturate the phosphate groups, the triplet decay profiles could be analyzed in terms of single-exponential fits. Under such conditions, diffusion of viologen

(21) The triplet energy for the various PdTMPyP(x) species in neutral aqueous solution is *ca.* 1.80 eV, as determined from the maximum of the phosphorescence spectra, while the one-electron reduction potential for MV^{2+} is −0.44 V vs NHE. The one-electron oxidation potentials for PdTMPyP(x) were found to be as follows: $x = 2$, $E° = 1.32$ V vs NHE; $x = 3$, $E° = 1.21$ V vs NHE; and $x = 4$, $E° = 1.41$ V vs NHE. Ignoring any corrections for changes in electrostatic potential that accompany electron transfer, the thermodynamic driving forces for light-induced electron transfer are $x = 2$, $\Delta G° = -0.04$ eV; $x = 3$, $\Delta G° = -0.15$ eV; and $x = 4$, $\Delta G° = +0.05$ eV.

(22) Darwent, J. R.; Douglas, P., Harriman, A.; Porter, G.; Richoux, M. C. *Coord. Chem. Rev.* **1982**, *44*, 127.

(23) Fromherz, P.; Rieger, B. *J. Am. Chem. Soc.* **1986**, *108*, 5361.

(24) Richoux, M. C.; Harriman, A. *J. Chem. Soc., Faraday Trans. 1* **1982**, *78*, 1873.

(25) Holten, D.; Windsor, M. W.; Parson, W. W.; Gouterman, M. *Photochem. Photobiol.* **1978**, *28*, 951.

(26) (a) Knochenmuss, R.; Gudel, H. U. *J. Chem. Phys.* **1987**, *86*, 1104. (b) Wieting, R. D.; Fayer, M. D.; Dlott, D. D. *J. Chem. Phys.* **1978**, *69*, 1996.

(27) Karlen, T.; Ludi, A.; Gudel, H. U.; Riesen, H. *Inorg. Chem.* **1981**, *30*, 2250.

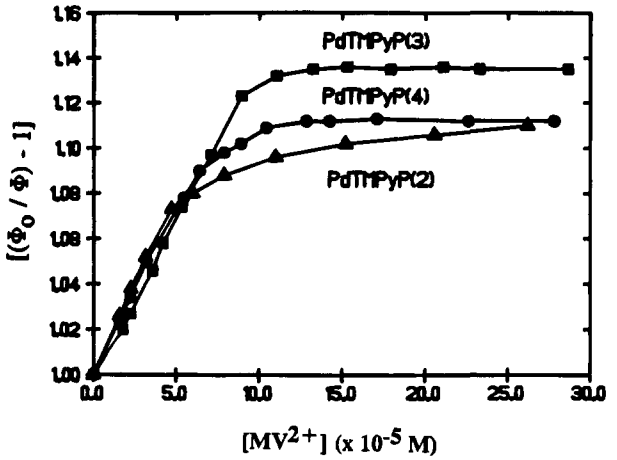

Figure 3. Effect of methyl viologen on the phosphorescence quantum yield measured for the various cationic palladium porphyrins bound to DNA at a P/D of 40. The concentration of DNA phosphate was 200 μM.

Table 4. Quenching of the Triplet Excited State of the Cationic Palladium Porphyrins by Methyl Viologen in DNA at a P/D = 40

x	$k_{max}/10^3$ (s^{-1})	$k_t/10^3$ (s^{-1})	$D/10^{-13}$ (cm^2 s^{-1})	k_m (s^{-1})
2	12.3	5.3	8.8	1100
3	2.9	1.2	1.1	930
4	0.84	1.4	1.5	950

along the phosphate backbone is inhibited and quenching of the porphyrin triplet occurs by electron transfer to a nearby viologen. The derived rate constants for electron transfer (k_t) were in excellent agreement with those calculated at lower loadings. For PdTMPyP(3) and PdTMPyP(4) increasing the viologen concentration above 100 μM did not further affect the triplet lifetime of the porphyrin, but for PdTMPyP(2) there was a decrease in triplet lifetime with increasing concentration of viologen beyond saturation. The bimolecular rate constant for this diffusional step ($k = (7.3 \pm 0.8) \times 10^8$ M^{-1} s^{-1}) was close to that determined from the steady-state phosphorescence studies.

Triplet Energy Transfer between Intercalated Reagents. Laser flash photolysis studies were undertaken in order to explore the possibility of triplet energy transfer from AO, which intercalates readily into DNA,[9] to PdTMPyP(3). From the respective low temperature phosphorescence spectra, triplet energy transfer was calculated to be exothermic by *ca.* 32 kJ mol^{-1}, while the triplet differential absorption spectra are sufficiently distinctive for proper evaluation of the energy transfer process (Figure 4a).

$$*^3AO + PdTMPyP(3) \rightarrow AO + *^3PdTMPyP(3) \quad (7)$$

AO absorbs at 355 nm where PdTMPyP(3) is relatively transparent and the resultant triplet excited state can be monitored at 490 nm. In deoxygenated aqueous solution, the AO triplet lifetime remained at (230 $\pm$ 20) μs regardless of the concentration of added PdTMPyP(3) ([PdTMPyP(3)] <30 μM). Thus, triplet energy transfer does not occur under these conditions, presumably because diffusion does not compete with inherent nonradiative deactivation of the AO triplet.[28]

Intercalation of AO (5 μM) into DNA (200 μM), which occurs with a binding constant of 2×10^6 M^{-1} and a saturation number of 2.0 base pairs,[29] increases the triplet lifetime to (700 $\pm$ 25) μs in the absence of O_2. Upon addition of PdTMPyP(3) (2 μM), the triplets of both AO and PdTMPyP(3) were observed following excitation at 355 nm with a 10-ns laser pulse (Figure 4b). Control experiments made in the absence of DNA indicated that PdTMPyP(3) does not compete effectively with AO for absorption of incident photons so that the porphyrin triplet must arise *via* energy transfer from AO. Kinetic studies showed that approximately 50% of the porphyrin triplet was formed within the 10-ns laser pulse, while the remainder appeared with a first-order rate constant of $(3.2 \pm 0.7) \times 10^4$ s^{-1} (Figure 4c). This latter process clearly corresponds to triplet energy transfer from AO to the porphyrin. Under these conditions, deactivation of the AO triplet occurred *via* nonexponential kinetics, but the

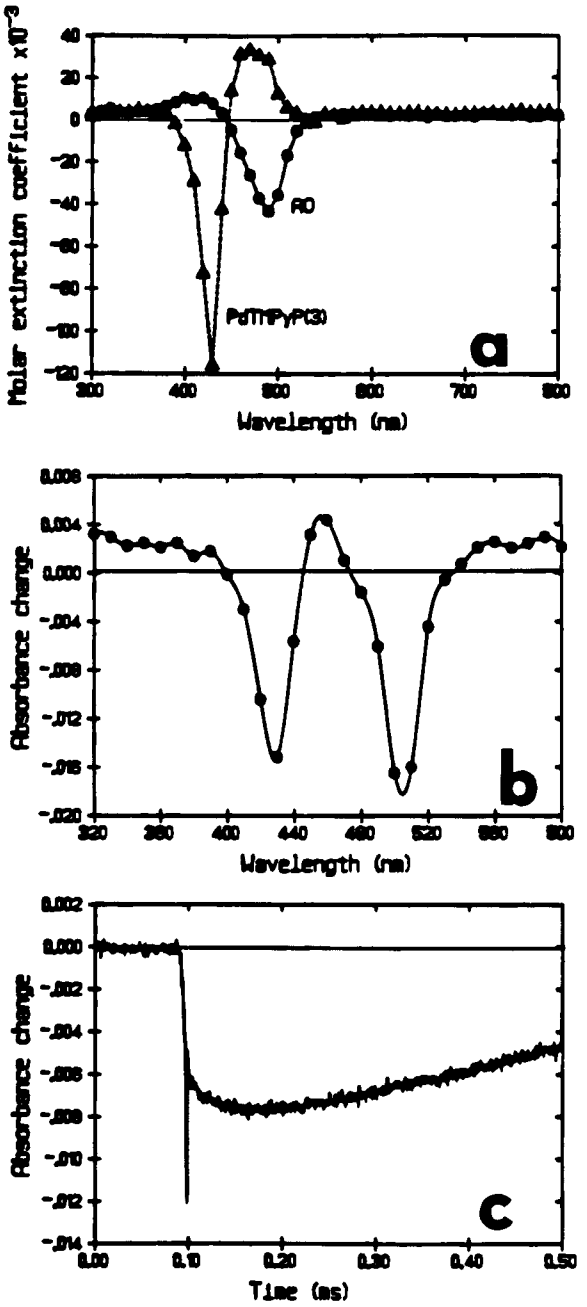

Figure 4. (a) Triplet differential absorption spectra recorded for AO (●) and PdTMPyP(3) (▲) intercalated separately into DNA (P/D = 40). The spectra were recorded 1 μs after the laser pulse. (b) Triplet differential absorption spectrum recorded 200 μs after laser excitation (355 nm) of AO (5 μM) intercalated into DNA (200 μM) in the presence of PdTMPyP(3) (2 μM). (c) Kinetic profile recorded at 430 nm for the experiment described in (b) above. All solutions were deoxygenated.

(28) Both the reactants are positively charged so that the diffusion-controlled rate limit is *ca.* 10^9 M^{-1} s^{-1}.

(29) Fredericq, F.; Houssier, C. *Biopolym.* **1970**, *9*, 639; **1972**, *11*, 2281.

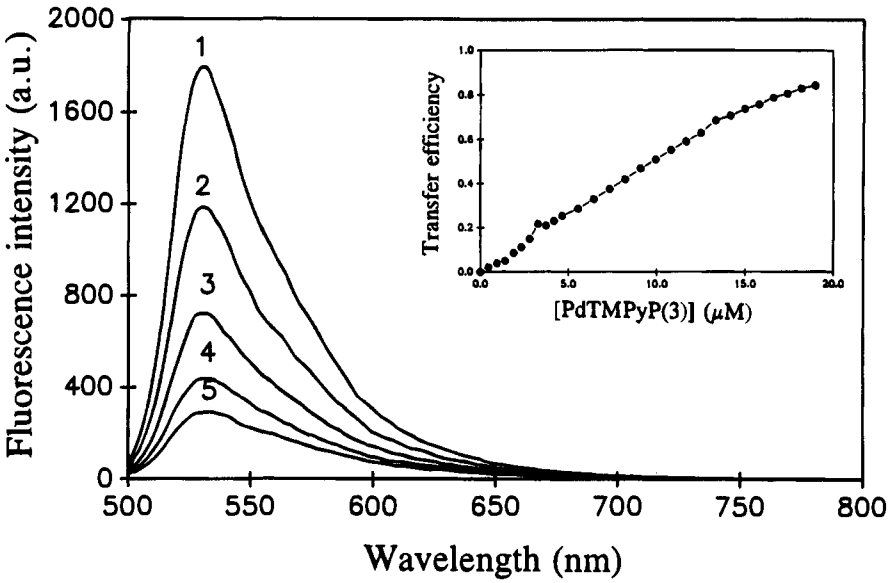

Figure 5. Effect of PdTMPyP(3) on the fluorescence spectrum of AO (5 μM) intercalated into DNA (200 μM); concentrations of PdTMPyP(3) are (1) 0, (2) 1, (3) 2, (4) 3, and (5) 5 μM. The inset shows a plot of transfer efficiency ($(I_o - I)/I_o$ where I and I_o refer, respectively, to the fluorescence quantum yields in the presence and absence of porphyrin) as a function of the concentration of PdTMPyP(3).

triplet was significantly shorter lived and its initial yield was substantially lower than found in the absence of PdTMPyP(3). The kinetic profiles were found to be independent of laser intensity and DNA concentration (keeping the same ratio of reactants).

Formation of triplet porphyrin on time scales shorter than 10 ns could be explained in one of two ways: First, rapid triplet energy transfer might occur between reactants in close proximity. In this case, the slow triplet energy-transfer step would correspond to transfer between remote reactants. Second, singlet electronic energy transfer might proceed from AO to porphyrin; such processes have been observed with several other couples intercalated into DNA[30] and might be expected to occur in view of the favorable spectroscopic properties of the reactants. Rapid singlet energy transfer would compete with intersystem-crossing to the AO triplet manifold and, thereby, would minimize triplet energy transfer between those couples. As such, triplet energytransfer would occur only for reactants that escape singlet energy transfer.

The observation of triplet energy transfer occurring over several tens of microseconds is of particular importance. This process must occur *via* a Dexter-type mechanism involving electron exchange. With both reactants intercalated into the same DNA duplex, electron exchange has to occur by way of the interspersed nucleic acid bases. Furthermore, as discussed above, triplet energy transfer must occur between spatially remote reagents. The poor precision of the kinetic data, however, precludes meaningful determination of rates of triplet energy transfer as a function of separation distance.

Singlet Energy Transfer Between Intercalated Reagents. To assess the importance of rapid singlet energy transfer in this system, a series of fluorescence studies were made. Adding small amounts of PdTMPyP(3) (0−5 μM) caused a progressive decrease in the fluorescence quantum yield of AO (5 μM) intercalated into DNA (200 μM) (Figure 5). However, emission from PdTMPyP(3) could not be detected under these conditions, probably because it lies underneath the residual emission of AO.[31] This quenching effect is consistent with singlet energy transfer from AO to PdTMPyP(3), which is exothermic by *ca.* 27 kJ mol^{-1}.

$$^{*1}\text{AO} + \text{PdTMPyP(3)} \rightarrow \text{AO} + ^{*1}\text{PdTMPyP(3)} \quad (8)$$

For energy transfer occurring *via* the Förster mechanism, the critical distance (R_0) can be calculated precisely according to

$$R_0^6 = \frac{8.8 \times 10^{-25} K^2 \Phi_F J_F}{n^4} \quad (9)$$

Here, K is an orientation factor, J_F is the spectral overlap integral, n is the refractive index of the medium, and Φ_F is the fluorescence quantum yield for AO intercalated into DNA but in the absence of quencher.[32] The fluorescence quantum yield was determined to be (0.67 ± 0.04) by comparison to quinine sulfate,[33] while K has a value of 1.0 for these reactants where the transition dipole moments lie parallel to each other and perpendicular to the connecting line.[34] The overlap integral was calculated[35] from comparison of normalized absorption and fluorescence spectra (Figure 6) and was found to be $J_F = 4.70 \times 10^{-17}$ cm^6 mmol^{-1}. On this basis, the critical distance is calculated to be 14.6 Å and indicates that Förster-type singlet energy transfer is highly favorable for intercalated reagents. In contrast, for the same concentration of reagents but in the absence of DNA there was no observable quenching of AO fluorescence.[36]

Alternate reasons for the observed diminution of AO fluorescence upon addition of PdTMPyP(3) include light-induced electron transfer or exclusion of AO from the duplex. From cyclic voltammetry measurements made with intercalated

(30) (a) Rayner, D. M.; Loutfy, R. O.; Szabo, A. G.; Yip, R. W. *J. Phys. Chem.* **1980**, *84*, 289. (b) Pasternack, R. F.; Giannetto, A.; Pagano, P.; Gibbs, E. J. *J. Am. Chem. Soc.* **1991**, *113*, 7799. (c) Baverstock, K. F.; Cundall, R. B. *Radiation Phys. Chem.* **1988**, *32*, 553. (d) Kaufmann, M.; Weill, G. *Biopolym.* **1971**, *10*, 1983. (e) Sutherland, J. C.; Sutherland, B. M. *Biopolym.* **1970**, *9*, 639.

(31) The total emission quantum yield for the various palladium porphyrins bound to DNA is <0.001 compared to the fluorescence quantum yield for AO of 0.67, as measured in the absence of PdTMPyP(*x*).

(32) Other researchers have reported fluorescence quantum yields for intercalated AO to be 0.87,[37] 0.75,[9c] and 0.72.[29]

(33) Meech, S. R.; Phillips, D. *J. Photochem.* **1983**, *23*, 193.

(34) Oevering, H.; Verhoeven, J. W.; Paddon-Row, M. N.; Cotsaris, E.; Hush, N. S. *Chem. Phys. Lett.* **1988**, *143*, 488.

(35) Sessler, J. L.; Capuano, V. L.; Harriman, A. *J. Am. Chem. Soc.* **1993**, *115*, 4618.

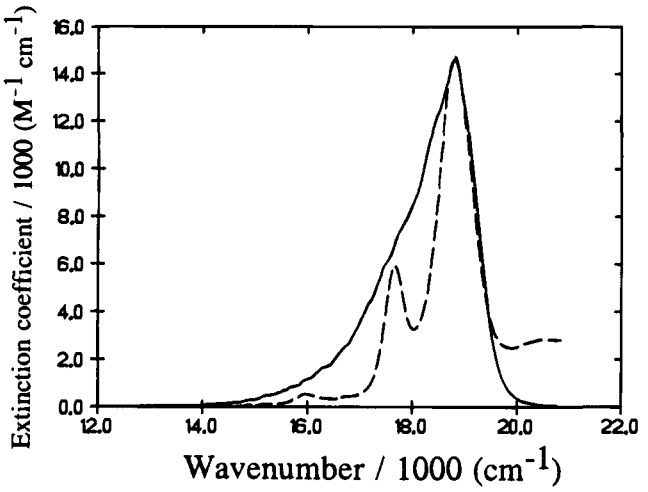

Figure 6. Spectral overlap between the fluorescence spectrum of AO (—) and the absorption spectrum of PdTMPyP(3) (– –) with both reagents intercalated into DNA at a P/D of 40.

reagents, the thermodynamic driving force for electron transfer to (ΔG° = +0.03 eV) or from (ΔG° = +0.02 eV) the excited singlet state of AO seems inconsistent with efficient fluorescence quenching *via* an electron-transfer mechanism. Furthermore, laser flash photolysis studies made with picosecond time resolution indicated that the relevant π-radical ions were not produced upon excitation of AO (10 μM) intercalated into DNA (200 μM) in the presence of PdTMPyP(3) (20 μM). With [AO] = 10 μM and a P/D of 20, about 99.7% of the dye will be intercalated into DNA. In order to effect a 50% reduction in the fluorescence yield for intercalated AO under such conditions, it is necessary to use a concentration of PdTMPyP(3) of 11.2 μM. From the known saturation numbers, this level of loading is not expected to exclude a significant amount of AO; it would require displacement of 40% of intercalated AO to account for a 50% reduction in the fluorescence yield if this was the only quenching mechanism. However, fluorescence excitation spectra clearly indicate that this is not the case since they correspond exactly with the absorption spectrum of intercalated AO. In addition, circular dichroism and gel electrophoresis studies indicate complete binding of AO to the DNA duplex under these conditions. It is most likely, therefore, that the observed fluorescence quenching arises from singlet energy transfer to intercalated PdTMPyP(3).

In order to determine rates of singlet energy transfer, time-resolved fluorescence profiles were recorded as a function of the concentration of PdTMPyP(3), keeping [AO] = 10 μM and [DNA phosphate] = 200 μM. In the absence of PdTMPyP(3), fluorescence decay profiles were monoexponential (Figure 7a) with a lifetime of (5.00 ± 0.05) ns, compared to a lifetime of (1.25 ± 0.05) ns recorded for AO in water. The observed fluorescence lifetime for intercalated AO is in excellent agreement with that reported by Weill.[37] Upon addition of PdTMPyP(3), fluorescence decay profiles were best fit by the sum of three exponential components

$$I_f(t) = A_1 \exp(-t/\tau_1) + A_2 \exp(-t/\tau_2) + A_3 \exp(-t/\tau_3) \quad (10)$$

even at low concentration of PdTMPyP(3) (Figure 7b). The

(36) Several factors combine to minimize the rate of energy transfer in fluid solution, including the shorter singlet excited state lifetime (τ = 1.25 ns), the lower fluorescence quantum yield (Φ_F = 0.25), and the smaller value for the orientation factor (K = 0.67).

(37) Weill, G. *Biopoly.* **1965**, *3*, 567.

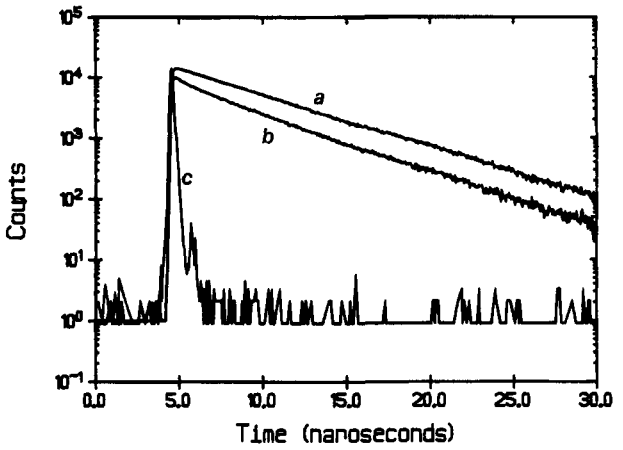

Figure 7. Fluorescence decay profiles recorded for AO (10 μM) in DNA (200 μM) recorded (a) in the absence and (b) in the presence of PdTMPyP(3) (10 μM). The instrumental response function is given as (c).

Table 5. Effect of PdTMPyP(3) on the Fluorescence Properties of AO (10 μM) Intercalated into DNA (200 μM)

[PdTMPyP(3)] (μM)	Φ/Φ_F[a]	$\tau_1(A_1)$ (ns)	$\tau_2(A_2)$ (ns)	$\tau_3(A_3)$ (ns)
0	1.00			5.00(100)
0.5	0.95	0.40(4)	2.23(5)	5.09(91)
1.0	0.86	0.39(9)	2.15(9)	4.85(82)
6.5	0.77	0.38(14)	2.07(14)	4.80(72)
9.1	0.60	0.38(22)	1.82(24)	4.68(54)
10.8	0.56	0.43(27)	1.95(26)	4.43(47)
11.7	0.42	0.31(34)	2.00(3)	4.15(36)
13.3	0.39	0.43(38)	1.97(31)	4.00(31)
15.0	0.40	0.42(38)	2.10(35)	3.92(27)
17.4	0.35	0.35(40)	1.88(36)	3.90(24)
19.0	0.32	0.38(42)	2.02(36)	3.90(22)

[a] Ratio of fluorescence yields measured in the absence (Φ_o) and presence (Φ) of PdTMPyP(3). For each derived lifetime (τ) the fractional contribution (A) is given in parentheses.

magnitude of the two shorter lifetimes (i.e., τ_1 and τ_2) remained independent of the concentration of added PdTMPyP(3), but their combined fractional contribution to the total signal (A_1 + A_2) increased with increasing concentration of quencher (Table 5). The averaged values for these two lifetimes, taken from several separate sets of data, were found to be τ_1 = (0.38 ± 0.06) and τ_2 = (2.0 ± 0.15) ns. Their relative fractional contributions (A_1 and A_2) remained comparable throughout the titration. Both the magnitude (τ_3) and the fractional contribution (A_3) of the longest lifetime decreased with increasing concentration of PdTMPyP(3) (Table 5). At low quencher concentrations, τ_3 remained similar to the unquenched lifetime but progressively decreased throughout the titration until reaching a lower limit of (3.9 ± 0.2) ns at the highest P/D. Comparison between steady-state and time-resolved fluorescence measurements indicated that there was not an additional fast component unresolved from the instrumental response function.

Following our earlier analysis of a related system,[4] the time-resolved fluorescence behavior can be explained as follows: At fixed loading of AO, intercalation of PdTMPyP(3) can occur at discrete distances from the incumbent AO. The separation between the two dyes cannot correspond to less than two interspersed base pairs (i.e., a center-to-center distance of 10.2 Å), because of mutual exclusion, but there will be a statistical distribution of individual separation distances, each a multiple of 3.4 Å. As the distance between intercalated molecules increases, the efficiency for energy transfer from the singlet state of AO decreases, and, as such, the derived fluorescence lifetimes

Table 6. Derived Fluorescence Lifetimes and Experimental Rate Constants for Energy Transfer over Different Numbers of Interspersed Base Pairs and the Corresponding Rate Constants Calculated for Förster- and Dexter-type Energy Transfer

[bp][a]	R (Å)	τ^b (ns)	k_{et} (s^{-1})	k_F (s^{-1})	k_D (s^{-1})
2	10.2	0.38	2.43×10^9	1.56×10^9	8.9×10^8
3	13.6	2.00	2.87×10^8	2.78×10^8	9.4×10^6
4	17.0	3.90[c]	5.60×10^7	7.28×10^7	9.8×10^4

[a] Number of interspersed base pairs. [b] Averaged over several sets of data. [c] As measured at high loadings of PdTMPyP(3).

can be attributed to rates of energy transfer over different distances. The experimental rate constants for energy transfer can be derived from the single-photon counting data as follows

$$k_{et} = (1/\tau) - (1/\tau_o) \tag{11}$$

where τ refers to one of the three lifetimes observed in the presence of PdTMPyP(3) and τ_o is the lifetime of intercalated AO observed in the absence of PdTMPyP(3) (Table 5). The shortest center-to-center separation between AO and PdTMPyP-(3), when both reagents are intercalated into DNA, corresponds to two interspersed base pairs (i.e., 10.2 Å). We assign, therefore, τ_1 to an AO molecule with the nearest PdTMPyP(3) molecule only 10.2 Å distant and τ_2 to an AO molecule with the neighboring PdTMPyP(3) molecule situated 13.6 Å away (Table 6). In the same manner τ_3, as observed at high concentrations of PdTMPyP(3), can be assigned to an AO molecule with the closest PdTMPyP(3) molecule removed by 17.0 Å . Further separation distances are possible, of course, but the rates of energy transfer would be too slow for this process to compete with inherent deactivation of the excited singlet state.

For predetermined separation distances, the rate of energy transfer occurring by the Förster mechanism (k_F) can be calculated from the following expression[10]

$$k_F = \frac{8.8 \times 10^{-25} K^2 \Phi_F J_F}{n^4 \tau_o R^6} \tag{12}$$

where the fluorescence lifetime of intercalated AO (τ_o) is equal to 5.0 ns, R is the mutual center-to-center separation distance, and the other parameters have been given earlier. The values calculated for various numbers of interspersed base pairs are shown in Figure 8, and selected values are provided in Table 6.

It is seen that there is very good agreement between the experimentally-derived k_{et} values and the calculated k_F values for separation distances of 13.6 and 17.0 Å (Table 6). This finding suggests that singlet energy transfer over large distances can be explained in terms of a Förster mechanism. At the closest approach, however, k_{et} exceeds k_F by an amount well outside the experimental uncertainty. This might indicate that mechanisms other than Förster-type energy transfer contribute to the overall process at short separations or that the Förster calculation is misleading at close approach of the reactants. The latter situation might arise if the actual separation distance is much less than 10.2 Å , due to distortion of the duplex, although this seems unlikely. Alternately, the orientation factor might be particularly favorable for closely-spaced reactants, again due to perturbation of the duplex.[38] The former situation would occur if energy transfer between reactants in close proximity involved both Förster and Dexter mechanisms. The occurrence of Dexter-type triplet energy transfer for this system is taken as support for the latter hypothesis.

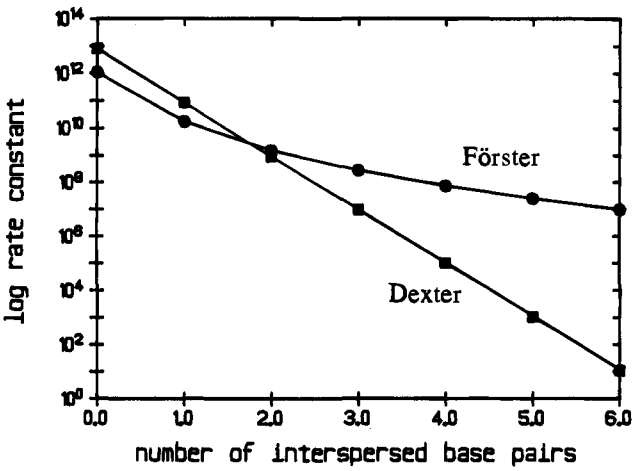

Figure 8. Effect of the number of interspersed base pairs on the calculated rate constants for singlet energy transfer from AO to PdTMPyP(3) according to Förster (●) and Dexter (■) mechanisms, with both reactants being intercalated into the duplex.

It is interesting to note that the Förster expression has been used to measure separation distances in tRNA and rRNA[39] and to measure the geometry of junctions in DNA.[40] Less satisfaction has been achieved in the application of the Förster equation to measure distances in oligonucleotides,[41] where it appears that the fluorescence quenching efficacy decreases less rapidly with increasing oligomer length than expected from theory. Other researchers have also shown that the Förster expression, when used with a common orientation factor, does not give a good representation of the distance dependence for intercalated reagents.[7c,42] These earlier studies, which mostly relied upon steady-state fluorescence data, were concerned with well-separated reagents, whereas, in our case, the anomolous behavior is observed at short separations. For closely-coupled systems, the R^{-6} dependence in the normal (i.e., weak interaction) Förster expression may not hold,[43] but we have not detected any spectral perturbation of the reactants that could be construed as evidence for strong electronic coupling. It seems likely, therefore, that an additional energy-transfer process becomes operative in our system at close approach of the intercalated reactants. Most probably this is due to the onset of Dexter-type energy transfer, although unexpectedly fast singlet energy transfer in photosynthetic light-harvesting antennae has been attributed to deficiencies in the Förster model when applied to strongly-coupled reagents.[44]

As such, the difference between observed and Förster rate constants for closely-spaced reagents is attributed to Dexter-type energy transfer. The calculated rate constant for Dexter-

(38) The orientation factor K will depend upon the number of interspersed base pairs (n) because the angle between the respective transition dipole moments (δ) varies according to $\delta = 2\pi n/10$. However, PdTMPyP(3) has two degenerate transition dipole moments such that the maximum value of K, for each value of n, will be less sensitive to separation distance. For intercalated reagents with $K = \cos \delta$, maximum values of K are calculated to be 0.95, 0.81, and 1.00, respectively, for n = 2, 3, and 4.

(39) (a) Beardsley, K.; Cantor, C. R. *Proc. Natl. Acad. Sci. U.S.A.* **1970**, *65*, 39. (b) Yang, C.-H.; Soll, D. *Proc. Natl. Acad. Sci. U.S.A.* **1974**, *71*, 2838. (c) Odom, O. W., Jr.; Robbins, D. J.; Lynch, J.; Dottavio-Martin, D.; Kramer, G.; Hardesty, B. *Biochemistry* **1980**, *19*, 5947. (d) Robbins, D. J.; Odom, O. W., Jr.; Lynch, J.; Kramer, G.; Hardesty, B.; Liou, R.; Ofengand, J. *Biochemistry* **1981**, *20*, 5301.

(40) Murchie, A. I. H.; Clegg, R. M.; von Kitzing, E.; Duckett, D. R.; Diekmann, S.; Lilley, D. M. *Nature* **1989**, *341*, 763.

(41) (a) Cooper, J. P.; Hagerman, P. J. *Biochem.* **1990**, *29*, 9261. (b) Cardullo, R. A.; Agrawal, S.; Flores, C.; Zamecnik, P. C.; Wolf, D. E. *Proc. Natl. Acad. Sci. U.S.A.* **1988**, *85*, 8790.

(42) Mergny, J.-L.; Slama-Schwok, A.; Montenay-Garestier, T.; Rougée, M.; Hélène, C. *Photochem. Photobiol.* **1991**, *53*, 555.

(43) Kenkre, V. M.; Knox, R. S. *Phys. Rev. Lett.* **1974**, *33*, 803.

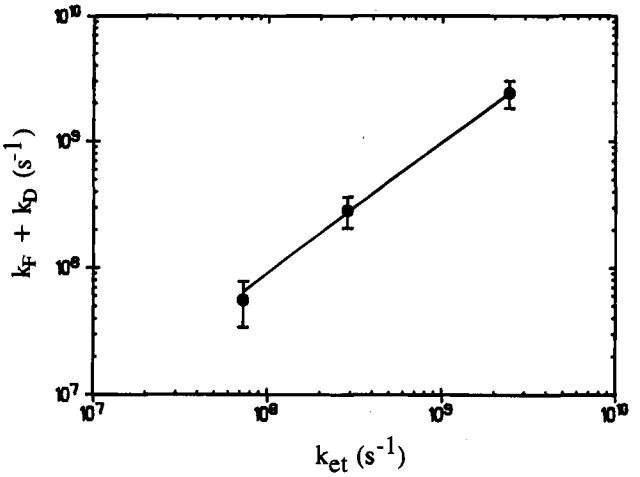

Figure 9. Comparison between the experimentally derived rate of energy transfer and the sum of the rate constants for Förster- and Dexter-type energy transfer at different separation distances.

type transfer (k_D) is 8.9×10^8 s^{-1} (Table 6).

$$k_{et} = k_F + k_D \tag{13}$$

This latter rate constant can be expressed in the form[11]

$$k_D = \frac{4\pi^2 H^2 J_D}{h} \tag{14}$$

where H is the electronic matrix coupling element and J_D refers to the Dexter spectral overlap integral. The overlap integral was determined to be 3.34×10^{-4} cm from comparison of normalized absorption and emission spectra, while, from evaluation of eq 14, H has a value of 2.1 cm^{-1}. It is expected that H decreases exponentially with increasing separation between the reactants according to

$$H = H_0 \exp[-\beta(R - 3.4)] \tag{15}$$

where the attenuation factor for electron exchange (β) can be approximated to the inverse of the Bohr radius ($\beta = 0.67$ $Å^{-1}$).[34] Therefore, k_D can be calculated for incremental numbers of interspersed base pairs and compared with the corresponding k_F values (Figure 8). According to this analysis, Dexter-type transfer is important only at short separations and as the mutual separation distance increases Förster-type transfer dominates. This situation mirrors the experimental data and appears to give an adequate description of the system. Indeed, there is an excellent correlation between the experimental rates (k_{et}) and the sum of the Förster and Dexter rates ($k_F + k_D$) as can be seen from Figure 9.

Concluding Remarks. The DNA double helix provides an ideal medium for assembling supramolecular systems in which photo- or redox-active molecules are intercalated into the strand. It is clear from this work that intercalated molecules are protected against reaction with molecular oxygen dissolved in the aqueous reservoir and with certain cations bound to the phosphate chain. In these latter systems, the polynucleotide serves to concentrate the reactants into a smaller reaction volume and to reduce the dimensionality, as has been reported previously.[23,45] Cations such as MV^{2+} or PdTMPyP(2) do not migrate rapidly along the phosphate chain,[23] and, even at contact, reaction is inefficient. Indeed, it must be emphasized that the rates of electron transfer decrease when one of the reactants is intercalated into the DNA strand compared to the same reactants dissolved in water.[45] The duplex does not promote (or accelerate) rates of electron transfer, at least for cases where the thermodynamic driving force is modest. It appears, therefore, that DNA does not provide a favorable environment for rapid electron transfer when one of the reactants is intercalated into the duplex but the other is not; except by virtue of concentrating the reactants.

Light-induced energy or electron transfer can occur between reactants that are both intercalated into the DNA duplex, and, in such cases, it becomes important to evaluate the capability of the medium to mediate the transfer process. As regards excitation energy transfer between intercalated reagents, the orientation is such that Förster-type singlet energy transfer is highly favorable. Indeed, with appropriate couples, molecular systems capable of long-range energy transfer could be engineered. Our experimental results, which are limited to only three discrete separation distances, can be explained precisely in terms of the Förster dipole–dipole mechanism only at relatively large separation of the reactants. Other researchers have also observed that the Förster mechanism fails to give a satisfactory description of the system when a range of separation distances is considered. Thus, Pasternack and co-workers[7c] have reported that, in the presence of DNA, porphyrins are effective quenchers of the first excited singlet state of ethidium bromide at a separation of 25–30 Å. This finding, which was attributed to intermolecular singlet energy transfer, and our current results appear to be in good agreement; the long fluorescence lifetime of intercalated ethidium (τ = 25 ns)[4] and excellent overlap between fluorescence and porphyrin absorption spectra should ensure a large Förster critical distance. Nonlinear Stern–Volmer plots observed by Pasternack *et al.* were explained in terms of the Perrin activated sphere model. It is difficult, however, to assess the physical significance of this model, especially when the apparent diameter of the activated sphere far exceeds the contact distance, and it has been postulated that the "efficiency of dipole coupling is raised at long distances".[7c] It must be recalled that although the angle between the transition dipole moments of intercalated reagents depends on the number of interspersed base pairs, this is not a severe problem for porphyrins because of their degenerate transition dipole moments.[38]

Other researchers have also reported that the Förster equation does not permit a quantitative description of singlet energy transfer along end-labeled oligonucleotides.[41a] Thus, oligonucleotides of varying length labeled at either end with fluorescein (donor) and eosin (acceptor) were observed to demonstrate efficient energy transfer, even with the chromophores separated by up to 20 base pairs. The quenching efficiency, obtained from steady-state fluorescence spectral measurements, decreased less rapidly with increasing oligomer length than was expected from the Förster equation. An additional, and extremely interesting, feature of this system concerns the observation[41a] that retaining the same number of interspersed base pairs but changing their composition affected the efficacy of energy transfer. This suggests specific interactions between dye and helix that complicate data analysis. Of course, in this case the dyes are not intercalated but remain free in solution.

Singlet energy transfer has also been described for a system comprising between intercalated *N,N'*-dimethyl-2,13-diazaperopyrenium (donor) and ethidium bromide (acceptor).[42] Intercalation of such a large donor seems certain to distort the helix, and, in fact, this dye exhibits complicated binding behavior.

(44) Jean, J. M.; Chan, C.-K.; Fleming, G. R. *Israel J. Chem.* **1988**, *28*, 169.

(45) Orellana, G.; Kirsch-de Mesmaeker, A.; Barton, J. K.; Turro, N. J. *Photochem. Photobiol.* **1991**, *54*, 499.

The Förster critical distance for this system was calculated[42] to be 38 Å. Time-resolved fluorescence decay profiles were markedly nonexponential, and the poor agreement between calculated and observed energy transfer efficacies was attributed to structural distortion of the duplex.

The foregoing discussion serves to illustrate that the basic Förster theory does not permit a satisfactory description of singlet energy transfer for reagents associated with oligo- and polynucleotides. There appear to be problems in fitting experimental data collected at both small and large separations, although no single data set exists that allows rigorous testing of the theory. Even more important than energy transfer in DNA is the issue concerning the ability of DNA to mediate long-range electron transfer between intercalated reagents. There is, in fact, indisputable evidence to indicate that such electron-transfer processes do take place. Indeed, rapid electron transfer has been observed between intercalated dyes and adjacent nucleic acid bases[46] and between intercalated redox-active species separated by <20 Å.[4] In this latter case, the attenuation factor (γ) describing the decrease in rate of electron transfer with increasing separation distance was found[4] to be *ca.* 0.9 $Å^{-1}$. Other researchers[6] have derived a particularly small attenuation factor ($\gamma < 0.2$ $Å^{-1}$) for electron transfer between transition metal chelates intercalated into end-labeled oligomers. These two contrasting estimates for α appear to indicate quite disparate capabilities of DNA to mediate long-range electron transfer. However, the nonhomologous nature of DNA,[47] different intercalation geometries, possibility of structural distortion accompanying intercalation, and poor definition of separation distances render detailed comparison of γ values somewhat premature.

We have reported here that triplet energy transfer occurs between AO and PdTMPyP(3) *via* an electron-exchange process. The minimum separation distance between the reactants in this case corresponds to three interspersed base pairs (i.e., a center-to-center distance of 13.6 Å). Treating the electron-exchange reaction in terms of Marcus theory[48] allows calculation of the electronic matrix coupling element[49] (V) as 0.04 cm^{-1}. Following the approach used by Barton *et al.*,[6] the attenuation factor for electron exchange in this system is estimated[50] to be *ca.* 1.8 $Å^{-1}$; assuming instead that the observed triplet energy transfer rate constant actually refers to reactants separated by four base pairs (i.e., 17.0 Å), γ would be *ca.* 1.4 $Å^{-1}$. These estimated values for α are comparable to the corresponding values derived for electron transfer in protein matrices[51] and, while being higher than our previous estimate[4] of $\gamma \approx 0.9$ $Å^{-1}$ found for electron transfer, greatly exceed that estimated for electron transfer through the core of oligionucleotides.[6] In short, all our available experimental evidence serves to indicate to us that DNA is not a good conductor for electron exchange involving widely-spaced, intercalated reagents.

Acknowledgment. We thank the N.I.H. for financial support of this work (GM 48150). The CFKR is supported by the University of Texas at Austin.

(46) (a) Brun, A. M.; Harriman, A. *J. Am. Chem. Soc.* **1991**, *113*, 8153. (b) Atherton, S. J.; Harriman, A. *J. Am. Chem. Soc.* **1993**, *115*, 1816.

(47) Risser, S. M.; Beratan, D. N. *J. Am. Chem. Soc.* **1993**, *115*, 2508.

(48) Vögtle, F.; Frank, M.; Nieger, M.; Belser, P.; von Zelewsky, A.; Balzani, V.; Barigelletti, F.; De Cola, L.; Flamigni, L. *Angew. Chem., Int. Ed. Engl.* **1993**, *32*, 1643.

(49) In making this calculation, the reaction driving force is assumed to be equal to the triplet energy gap (i.e., −0.33 eV) and the reorganization energy is estimated as 0.2 eV (see ref 48). The calculation also demands that the observed rate constant for triplet energy transfer ($k = 3.2 \times 10^4$ s^{-1}) refers to electron exchange over a specified edge-to-edge separation distance (i.e., 10.2 Å).

(50) This calculation was made according to $k = k_o \exp[-\gamma(R_{cc} - 3.4)]$ where k is the observed rate constant for triplet energy transfer ($k = 3.2 \times 10^4$ s^{-1}) and k_o is the rate constant with no interspersed base pairs. The center-to-center separation distance is assumed to be 13.6 Å (the text also allows for $R_{cc} = 17.0$ Å). It is assumed that $k_o \approx 1 \times 10^{13} \exp[-\Delta G^*/RT]$ where the activation free energy change ($\Delta G^* = 0.021$ eV) is estimated from Marcus theory with the parameters given in ref. 49.

(51) (a) Beratan, D. N.; Betts, J. N.; Onuchic, J. N. *Science* **1991**, *252*, 1285. (b) Siddarth, P.; Marcus, R. A. *J. Phys. Chem.* **1993**, *97*, 6111.